Direct fabrication of homogeneous microfluidic channels embedded in fused silica using a femtosecond laser

Fei He,[1,2] Ya Cheng,[1,5] Zhizhan Xu,[1,6] Yang Liao,[1,2] Jian Xu,[1,2] Haiyi Sun,[1] Chen Wang,[1] Zenghui Zhou,[1] Koji Sugioka,[3] Katsumi Midorikawa,[3] Yonghao Xu,[4] and Xianfeng Chen[4]

[1]*State Key Laboratory of High Field Laser Physics, Shanghai Institute of Optics and Fine Mechanics, Chinese Academy of Sciences, P.O. Box 800-211, Shanghai 201800, China*
[2]*Graduate School of the Chinese Academy of Sciences, Beijing 100039, China*
[3]*Laser Technology Laboratory, RIKEN-Advanced Science Institute, Hirosawa 2-1, Wako, Saitama 351-0198, Japan*
[4]*Institute of Optics and Photonics, Department of Physics, Shanghai Jiao Tong University, 800 Dongchuan Road, Shanghai 200240, China*
[5] *ycheng-45277@hotmail.com*
[6] *zzxu@mail.shcnc.ac.cna*

Received October 20, 2009; revised December 9, 2009; accepted December 14, 2009; posted December 23, 2009 (Doc. ID 118812); published January 21, 2010

We demonstrate direct fabrication of homogeneous microfluidic channels embedded in fused silica by femtosecond laser direct writing, followed by wet chemical etching and glass drawing. In addition, the glass drawing process significantly reduces the inner surface roughness of the fabricated channels, and centimeter-level microfluidic channels with an aspect ratio above 1000 can be realized. © 2010 Optical Society of America

OCIS codes: 140.3390, 140.7090, 160.2750, 270.4180, 350.3390.

The development of microfluidic devices and micro-total analysis systems (μ-TASs) has attracted broad attention in the fields of chemical and biological analyses [1]. Currently, the fabrication of the μ-TAS with three-dimensional (3D) configurations usually requires a multilayer and multistep processing (e.g., stacking and fusing substrates) [2]. Recently, femtosecond laser micromachining has been proved to be an alternative way for creating 3D microstructures inside transparent materials [3–11]. Generally, the microchannels fabricated by femtosecond laser microfabrication followed by a chemical etching tend to display a tapered feature. This is due to the limited contrast ratio (typically 30–50) of etching selectivity between the laser exposed and unexposed regions. Since the chemical etching always begins from the surface of the substrate and progresses toward the middle areas of the channels, the regions close to the opening will always suffer a longer etching period as compared to the middle regions. This issue becomes even worse for fabricating long channels with lengths up to a few millimeters. Moreover, the microchannels fabricated by a femtosecond laser typically exhibit a high roughness of their inner surfaces, which is often undesirable for both microfluidic and optofluidic applications. In this Letter, we show that the fabrication of homogeneous microfluidic channels with smooth inner surfaces can be achieved by applying a post-etching glass drawing process.

In this work, commercially available fused silica is cut into 5 mm × 10 mm × 1 mm coupons with the upper and lower surfaces polished. The femtosecond laser (Coherent, Inc.) emits 800 nm 40 fs pulses with a maximum pulse energy of ~2.5 mJ at a 1 kHz repetition rate. The initial 8.8 mm diameter beam is reduced to 5 mm by a circular aperture so as to guarantee a high beam quality. A 20× objective with an NA of 0.46 is employed for focusing the beam. The energy of the beam is varied by a neutral density filter. The glass samples can be translated by a personal-computer-controlled *XYZ* stage with a resolution of 1 μm. The average femtosecond laser power is chosen to be 20 mW, and the translating speed of the stage is 30 μm/s. In addition, for facilitating the glass drawing process, two dents with a size of 1 mm × 1 mm are symmetrically fabricated near the Y-shaped microchannel structure as shown in Fig. 1(a). The dents are fabricated by scanning the focused laser beam along the edges of the dents layer by layer at a laser power of 30 mW and a scanning speed of 667 μm/s. The vertical spacing between two adjacent layers is 15 μm. The total time to fabricate these two dents is ~15 min.

After the femtosecond laser exposure, the sample is subjected to a 4 h ultrasonic bath in a solution of 10% HF diluted with water, until the microchannels and the two dents are formed. Figure 1(a) shows a schematic view of the 3D Y-shaped microchannel embedded 500 μm beneath the surface of the fused silica. The total length and width of the Y-shaped channel structure are 1400 and 600 μm, respectively. A micrograph of the fabricated Y-shaped channel structure is shown in Fig. 2(a). Then we fix the two ends of the

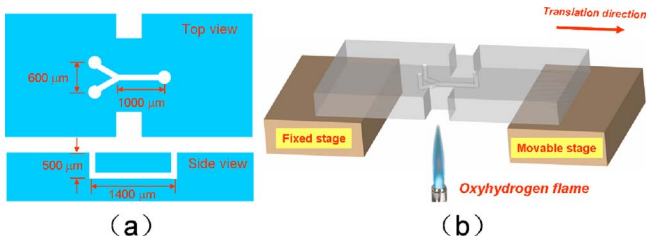

Fig. 1. (Color online) Schematic view of (a) the 3D microfluidic channel and (b) the glass drawing setup.

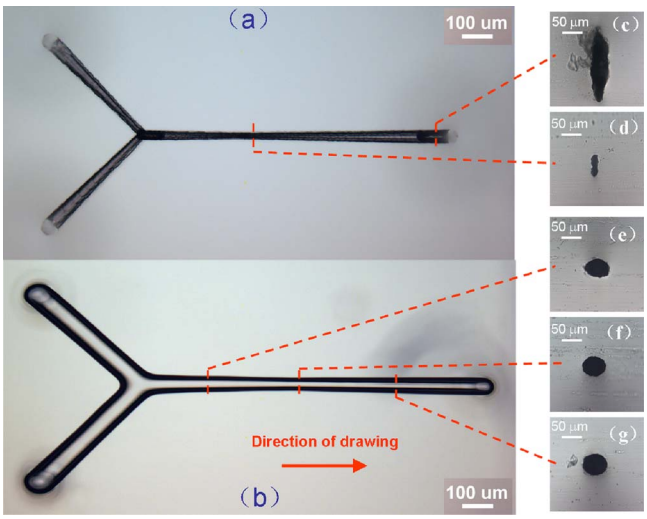

Fig. 2. (Color online) Optical micrographs of the Y-branched channels. Top view of the channels (a) before and (b) after drawing, and (c)–(g) cross section view of the channels at the locations indicated by the cutting lines.

fabricated sample on two stages, as illustrated in Fig. 1(b). Next, the sample is heated with an oxyhydrogen flame (JD90, Zhengzhou, China). The diameter of the flame is ~0.5 mm, which is determined by the nozzle size of the oxyhydrogen flame. The temperature on the glass sample is estimated to be close to the melting point of the fused silica (~1700°C). Since the glass sample is softened under such a high temperature, we can draw the glass sample in a direction parallel to the 1000-μm-long microfluidic channel by translating one of the two stages while fixing the other. Although different drawing parameters have been tested, we found that the optimum drawing speed is 1 μm/s, and a homogeneous channel can be obtained with a drawing length of ~200 μm (e.g., the movable stage is translated by 200 μm).

For comparison, Figs. 2(a) and 2(b) show both the optical micrographs of microfluidic channels before and after the drawing process, respectively. It can be seen in Fig. 2(a) that before drawing, the taper of the fabricated microfluidic channel is severe. Also the cross-section view of the channel clearly shows a highly elliptical shape, which is caused by the lower longitudinal resolution of an objective as compared to its transverse counterpart [6]. Interestingly enough, the channel width tapering is significantly reduced after the glass drawing as shown in Fig. 2(b). For the 1000-μm-long microfluidic channel, its taper angle is reduced from ~4.2° to ~0.8°. It can also be seen that the cross section of the channel shows a nearly circular shape after the drawing. Specifically, we examine the cross sections of the channel at three different locations as indicated by the cutting lines in Fig. 2(b), and we find that their dimensions are close to each other.

To test whether this technique could be applicable for microfluidic channels oriented unparallel with respect to the direction of glass drawing, we fabricate a T-shaped microchannel structure and examine the cross section of the vertical channel as shown in Figs. 3(a) and 3(b). It is found that the taper angle of the

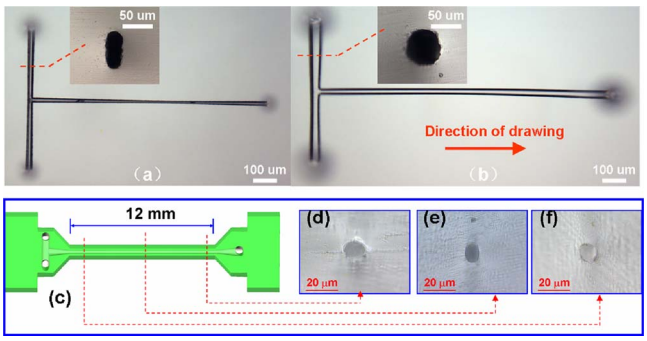

Fig. 3. (Color online) Top-view micrographs of T-shaped channels (a) before and (b) after drawing. (c) Schematic drawing of a 12-mm-long channel. (d)–(f) Cross sections at the different locations indicated by the cutting lines.

vertical channel remains to be ~1.2° even after the drawing, indicating that drawing must be carried out along the channel direction for creating the homogeneous channel. However, we also found that the drawing process can still reshape the initially elliptical cross section of the vertical microchannels into the circular one. In addition, with this technique it is possible to fabricate channels with a very high aspect ratio (channel length divided by diameter) by further drawing a 1-mm-long microchannel to a total length of ~12 mm. After drawing, the microchannel shows a uniform diameter of ~10 μm in Fig. 3(c), indicating an aspect ratio above 1000.

Furthermore, in order to examine the inner surface after the drawing, we polish the samples until the microchannels are exposed. Compared in Figs. 4(a) and 4(b) are, respectively, the scanning electron microscopic (SEM) images of the inner surfaces of microfluidic channels before and after the glass drawing. The cracks at the edges of both channels in Figs. 4(a) and 4(b) are caused by polishing. It is clear that, before the glass drawing, the inner surface roughness is high, which is consistent with the results reported before [11,12]. However, after the glass drawing process, the inner surface of the microfluidic channel becomes very smooth. To quantitatively investigate the roughness improvement, scanning-probe micrographs (SPMs) of the inner surfaces fab-

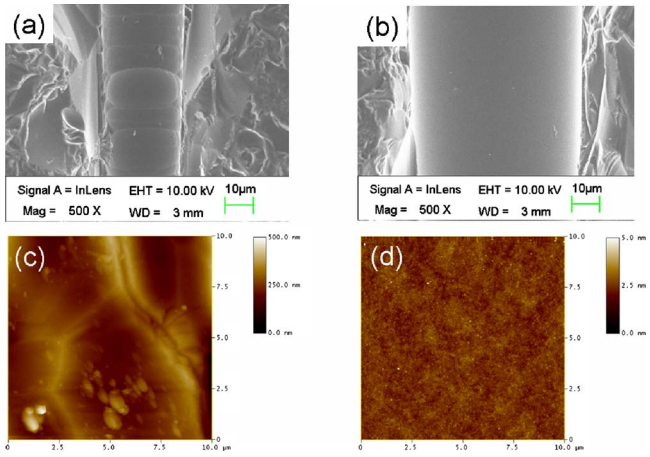

Fig. 4. (Color online) SEM images of the inner surfaces (a) before and (b) after drawing, and SPMs of the etched inner surfaces (c) before and (d) after drawing.

ricated without and with the drawing process are compared in Figs. 4(c) and 4(d), respectively. In this case, flat inner surfaces are required for the SPM scanning; therefore, we fabricate two microchannels with a rectangular cross section under the same experimental conditions. One of the microchannels undergoes the glass drawing, while the other does not. As one can see in Table 1, the root-mean-square (RMS) roughness (R_q) of the inner surface of the microchannel is greatly reduced from 50.3 to 0.29 nm with the drawing process. Such a high smoothness may offer opportunities in applications of the μ-TAS and optofluidics.

The mechanism of the channel reshaping is tentatively proposed as follows. Under the heating by oxyhydrogen flame, the fused silica will reach a high temperature above the softening point and will form a liquidlike phase. For liquid, its shape will be strongly influenced by the surface tension. Therefore, the microfluidic channel embedded in the molten glass will naturally transform itself into a homogenous channel with a uniform diameter and a circular cross section. This is because for a microchannel with a fixed length, its inner surface area and, consequently, the surface energy will be minimized if the channel has a round-shaped cross section and a uniform diameter. It should be pointed out that the surface tension alone is not strong enough to induce the reshaping of the microfluidic channel because we have observed that, if we heat only the glass sample on the stationary stage without drawing it by a certain amount of length, the fabricated channels will still remain tapered. Further investigation is required to fully understand the mechanism behind this phenomenon.

In conclusion, we have demonstrated a modified femtosecond laser microfabrication technique for fabricating 3D microfluidic channels embedded in a fused silica with excellent homogeneity and surface smoothness. Further refinement of this technique may enable the fabrication of nanochannels, which may find applications in single molecule detection [13]. The capability of fabricating homogenous channels using femtosecond laser microfabrication opens up a broad spectrum of opportunities for future microfluidic and optofluidic applications.

Table 1. Comparison of the RMS Roughness (R_q), Average Roughness (R_a), and Maximum Roughness (R_{max}) Before and After Drawing

Sample	RMS (R_q) (nm)	R_a (nm)	R_{max} (nm)
Before drawing	50.3	40.4	455.3
After drawing	0.29	0.22	7.6

This work is supported by the National Basic Research Program of China (grant 2006CB80600). Y. Cheng acknowledges the National Outstanding Youth Foundation.

References

1. K. Sato, M. Tokeshi, T. Kitamori, and T. Sawada, Anal. Sci. **15**, 641 (1999).
2. J. Zaumseil, M. A. Meitl, J. W. P. Hsu, B. R. Acharya, K. W. Baldwin, Y. L. Loo, and J. A. Rogers, Nano Lett. **3**, 1223 (2003).
3. A. Marcinkevičius, S. Juodkazis, M. Watanabe, M. Miwa, S. Matsuo, H. Misawa, and J. Nishii, Opt. Lett. **26**, 277 (2001).
4. M. Masuda, K. Sugioka, Y. Cheng, N. Aoki, M. Kawachi, K. Shihoyama, K. Toyoda, H. Helvajian, and K. Midorikawa, Appl. Phys. A **A76**, 857 (2003).
5. Y. Cheng, K. Sugioka, K. Midorikawa, M. Masuda, K. Toyoda, M. Kawachi, and K. Shihoyama, Opt. Lett. **28**, 55 (2003).
6. C. Hnatovsky, R. S. Taylor, E. Simova, V. R. Bhardwaj, D. M. Rayner, and P. B. Corkum, Opt. Lett. **30**, 1867 (2005).
7. V. Maselli, R. Osellame, G. Cerullo, R. Ramponi, P. Laporta, L. Magagnin, and P. L. Cavallotti, Appl. Phys. Lett. **88**, 191107 (2006).
8. Y. Li, K. Itoh, W. Watanabe, K. Yamada, D. Kuroda, J. Nishii, and Y. Jiang, Opt. Lett. **26**, 1912 (2001).
9. Y. Cheng, K. Sugioka, and K. Midorikawa, Opt. Lett. **29**, 2007 (2004).
10. K. C. Vishnubhatla, N. Bellini, R. Ramponi, G. Cerullo, and R. Osellame, Opt. Express **17**, 8685 (2009).
11. Y. Cheng, K. Sugioka, K. Midorikawa, M. Masuda, K. Toyoda, M. Kawachi, and K. Shihoyama, Opt. Lett. **28**, 1144 (2003).
12. Y. Bellouard, A. Said, M. Dugan, and P. Bado, Opt. Express **12**, 2120 (2004).
13. T. P. Burg and M. Godin, Nature **446**, 1066 (2007).